Optical Spectroscopy of GLIMPSE Stars with 8 Micron Infrared Excess

Authors:

Georgi Chunev (Manchester College), Sarah Bird (Missouri University),
Chip Kobulnicky , and Brian Uzpen (University of Wyoming)

Mentor:

Christer Watson

Manchester College, 2008

Abstract:

Advances in telescope sensitivity and angular resolution are opening the way for new approaches to the search for extrasolar terrestrial planets. When direct observation is not possible, as is often the case, a solution to the problem is identifying stars with debris disks (a signature for planetary formation) based on photometric and spectral data. In our study, Spitzer GLIMPSE (3.6, 4.5, 5.8, and 8.0μm) and 2MASS (at 1.3, 1.7, and 2.2μm) photometry was used to identify about 450 middle-range temperature (classes A or B) stars in our galaxy, having excess emission at 8.0μm. Among several possibilities, one source of the excess emission could be the presence of a debris-disk. To rule out, or confirm, other causes of the observed infrared excesses, optical spectra (3910 - 6660 Å) for a subset of 23 stars were obtained with the Wyoming Infrared Observatory's (WIRO) 2.3m telescope and longslit spectrograph. The spectra were used to classify the stars, which gave insight into the evolutionary stage of each source and confirmed the accuracy of our selection criteria (class A and B stars). Finally, the presence of Balmer alpha (Hα) emission lines in some of the collected spectra suggested that ionized gas, as opposed to dust and planetary debris, is the cause of 8.0μm emission excess for these sources. From the 23 observed stars four exhibited Hα emission; six were too evolved; and 13 had all the necessary characteristics to still be considered candidates for young systems with warm massive dust disks – associated with terrestrial-type planetary formation.

Background and Introduction:

The goal of our study is to combine photometric and spectral data to identify stars in our galaxy that are candidates for having warm debris disks around them, indicating ongoing planetary formation – a process, which occurs early in the life of some stars.

A Star is formed through the gravitational collapse of a rotating, interstellar, gaseous (mostly hydrogen) cloud. As the cloud collapses it forms a central source (the future star), and a circumstellar disk – comprised of particles away from the axis of rotation, i.e. the ones with largest angular momentum. Protostars of mass less than 8 solar masses (the mass range of stars around which we can expect to find terrestrial type planets) are thought to evolve solely through accreting material from their circumstelar disk. Thus, by the time these stars have entered the main sequence (another way of saying that a star is formed, has enough hydrogen fuel, and is efficiently fusing it) a large portion of the circumstellar disk has been accreted onto the central source, another part has evaporated, and yet another part could be forming planetary material. In the case of protostars, all three of these processes can broadly be defined as the occurrence of disk clearing – a process, which we consider to be over as soon as all ionized gas has been blown away from the circumstellar disk. Once disk clearing is over the star is formed and we can talk about the possibility of ongoing planetary formation, which due to asteroidal collisions will develop a warm debris disk around the newly born star.

It should be noted that there is a difference between protoplanetary disks, which are dusty remnants of a protostar's circumstellar disk, and debris disks, which are the result of scattered material from the collisions of already formed planetesimals that surround a star at a given orbit. Nevertheless, both disks (belts) are relevant to planet formation, and thus it is not a problem that in this work we do not distinguish between them.

We are more concerned with distinguishing disks that are forming Earth-like planets from ones forming objects like Pluto. As can be seen from Figure 5, if we use a

black body emission curve to approximate the strength of emission at different wavelengths (or the spectral energy distribution, SED) for an Earth-like object we should find peak emission at about 10μm and no emission below 3μm. Thus, in a warm debris disk system, where the SED is a composition of the SED of the central star with the SED of the debris disk, there will be two peaks in emission. To identify the presence of a second emission peak (the excess mid-IR emission) at terrestrial temperatures (~300K) we use the GLIMPSE (Benjamin, 2003) and 2MASS integrated fluxes, which essentially give us the values of a star's SED at the following wavelengths: (1.3, 1.7, 2.2, 3.6, 4.5, 5.8, and 8.0μm). High ratios between the longer-wavelength (also called redder) fluxes and the shorter-wavelength (bluer) fluxes define the presence of excess emission. At this stage, there is no guarantee that the excess emission is caused by a debris disk, thus we further investigate the possible source of the MIR excess through previously tested data analysis techniques and more observations.

As mentioned above, the first step in identifying potential debris disk candidate sources with our technique is to observe excess emission in the mid-infrared, using publicly available photometric data. In particular, we use the GLIMPSE galactic survey, which provides an open Point Source Catalogue with integrated fluxes (measures of total brightness) for four of the Spitzer Space Telescope IRAC wavebands along with the data from a previous galactic survey, 2MASS. The 2MASS bands *J*, *H*, and *K*, are defined in the Johnson photometric system (Norton, 2004, p. 63) and are centered at 1.25, 1.65, 2.2μm respectively, while the IRAC bands [3.6], [4.5], [5.8], and [8.0] are centered at slightly longer wavelengths. Each band has a width chosen to capture specific line

features, which, in our case, are relevant to identifying the source of mid-infrared excess for some of our stars.

We are looking for very young stars (ones that are forming planets), and it is known that the environment in which stars form is often dominated by certain types of polycyclic aromatic hydrocarbons (PAHs). These compounds absorb and re-emit light within the 3.6, 5.8, and 8.0μm bands, and, if present, would contribute to the mid-infrared excess emission. Note, that [4.5] is devoid of PAH emission (Mulas, 2005, Fig. 2), therefore it is suitable for identifying mid-IR excess stars. One problem with [4.5] is that it includes the Brackett alpha emission line at 4.05 ± .03 μm (Brackett, 1922), which contributes to excess emission in classical emission line stars – sources that we want to filter out from our set. We fix this problem by discarding sources that exhibit emission at Balmer alpha (Hα), which is a line we observed with WIRO.

Since, IRAC's highest resolving power is for the [8.0] band, and due to the above mentioned [4.5] band characteristics, we chose to define mid-IR excess using [4.5] and [8.0]. As a continuation of our study it would be interesting to explore to what extent the sources in our candidate set exhibit excess emission at other wavelengths. In particular, 24μm data, which is also devoid of strong PAH emission and will be available through the MIPS survey, would be useful, but for now [4.5] and [8.0] suffice. Actually, GLIMPSE data is given in magnitudes, which are defined as: $-2.5\log_{10}(F)$, where F is the flux (here a measure of total luminosity at a given wavelength) that we are concerned with. (Norton, 2004, p. 63) Since we want a measure of the ratio of the 8.0μm flux to the 4.5μm flux for a given source we have to use the difference between the [4.5] and [8.0] GLIMPSE fluxes:

$$-2.5\log_{10}(F(8.0)/F(4.5)) = -2.5\log_{10}(F(8.0)) + 2.5\log_{10}(F(4.5)) = [4.5] - [8.0]$$

When fluxes are given in magnitudes, differences between them are called colors. In that sense, our selection is based on color criteria.

To eliminate photometric errors and increase the likelihood of finding real circumstellar excess we take sources whose [4.5] – [8.0] color is greater than 0.2. Also, based on the colors of the debris disk candidates found by Brian Uzpen in his previous studies (Uzpen et al. 2005, 2007) and on the fact that some Class II protostars (protostars with a circumstellar accretion disk) exhibit [4.5] – [8.0] color as low as 0.8, we chose to reject sources with [4.5] – [8.0] color greater than 0.8.

We can also pre-select our sources, based on their *J-K* color, so that they fall within a desired range of spectral classes. The standard spectral classification scheme (Keenan et al. 1973) is based on temperature, and in the most general case separates stars into the following spectral types: O B A F G K M, with O stars being the hottest ones. With the advancement of technology (better spectral resolutions) these classes keep being refined – for instance a B2 star (also called an early B star) is hotter than a B7, or late B, star. For the purpose of our study we want to select sources similar to Beta Pictoris (the prototype debris disk star, Sp. Class A5), and to the ones already found by Uzpen (Uzpen et al. 2005, 2007), which were mostly late B and early A stars that exhibited *K*-[8.0] excess emission. A color criterion for selecting stars from these spectral classes, and minimizing the chances of selecting Class II protostars (as can be seen from Fig. 1), is to have $-.03 < J-K < 0.25$, which when combined with the previously stated [4.5] – [8.0] criterion allows us to define a narrow region of *J-K* vs. [4.5] – [8.0] color-color space.

Finally, we want to be able to distinguish candidates for early main sequence, planet-forming stars from late protostars undergoing disk clearing. Objects that fall into the final stage of star formation are of interest, but are beyond the scope of our work. For our purposes we want to filter out all sources that exhibit evidence for ionized gas, be it protostars, or classical Be stars (emission line stars that have MIR excess and could be present in our sample). A signature of ionized gas is the presence of Hα emission, which we can observe with WIRO. We do not further investigate the possible cause of Hα emission, but simply reject all sources that exhibit it, knowing that debris disk candidates should be devoid of ionized gas.

Our work is a continuation of what has previously been done and published by graduate student Brian Uzpen at the University of Wyoming (Uzpen et al. 2005, 2007). After collecting visual spectra for a subset of 170 stars (Uzpen et al. 2005) from the GLIMPSE observation strategy validation (OSV) region, which is a relatively small patch on the sky, Uzpen confirmed the presence of 18 warm debris disk candidate sources in the region (see Fig. 1), and suggested that it is worthwhile to look for such sources through the entire GLIMPSE survey (31 million Milky Way stars) – which is what our project aims at. To filter out protostars and evolved stars from the entire source set, only stars with identified spectral types can be considered, thus Uzpen used data form the Tycho-2 Spectral Catalogue to narrow down the set to about 33,000 sources (Uzpen et al. 2007). After further studies, only 23 stars exhibited the characteristics that Uzpen was looking for (Uzpen et al. 2007). One reason for the small size of the resulting subset is the weaker sensitivity of Tycho-2 compared to GLIMPSE, which caused most of the potential candidate sources not to be considered. Here we present WIRO longslit spectral

observations of 23 of these stars; the identified spectral classes for these sources; and our analysis of the results.

Data and Observations:

Due to the narrowness of our selection region we are left with only 449 sources (see Fig. 2) out of the 15.9 million GLIMPSE objects in the northern hemisphere. Collecting the visual spectra of the candidate debris disk sources is essential for our project; however, WIRO can not observe southern sources, which is why we considered only half of the GLIMPSE objects. Still, it is surprising that so few GLIMPSE sources exhibit the color criteria we posed; therefore we are hoping that these objects are undergoing a rapid transition phase in stellar evolution – which would be the case for planet forming stars or for protostars in the last stage of their formation.

The final data we needed, to carry out our analysis, were the optical spectra (3910 - 6660 Å) of the candidate sources. Due to time constraints and calibration issues we were able to collect the spectra of only 23 of the initial 449 sources (see Fig. 2). We got to do three runs at WIRO in the summer of 2007, each of which lasted for a full night. We used the WIRO Long-Slit instrument, which is a low resolution spectrograph, designed for efficient spectroscopy of faint sources. Because of the characteristics of WIRO and since there is chance that the brightest stars on our list have already been observed and classified, we gave preference to dimmer sources. Actually, 3 of the stars we selected for observation had classifications listed in Simbad (an online database), but they differed form our results. There can be several explanations for this, one of which is that the Simbad classifications could have been done with instruments having a lower spectral resolution. We used different dispersive gratings for the red and blue sections of our

spectra, which in some sections of the collected spectra allowed us to distinguish line features 1.5 Å apart from each other (this was our highest spectral resolution). We reduced (cleared from noise) and continuum normalized all of our spectral data using the IRAF data reduction package. Further modifications of the data, as well as most of its analysis, we did using our own, custom-built IDL tools.

Results:

We assigned a spectral and luminosity class for each star by comparison with standard stellar atlases (e.g., Silva & Cornell 1992). Figure 4 shows the optical spectra for a representative sample of 10 observed objects. The spectral classification scheme was briefly discussed in the previous section, where we mentioned that it is based on temperature. The proportions of the different accessible excitation states for the elements present in a stellar atmosphere vary with temperature, thus yielding different ratios between the strengths of the observed absorption lines resulting from each element. For instance, the abundance of hydrogen at its second lowest excitation level in a stellar atmosphere peaks at about 11,000K (Keenan et al. 1973), which is the temperature for type A0 stars, thus the spectrum of an A0 star has the strongest Balmer lines.

On the other hand, luminosity classes are not dependent on temperature, but are based on the strength of gravity on the surface of a given star. The stronger the surface gravity of a star, the wider will its spectral lines appear, due to a strong stretching effect. We already mentioned that when stars form they enter what is called the main sequence – it is defined as luminosity class V, and stars that fall into it are referred to as dwarfs. As stars age, the balance between the gravitational force, which contracts them, and the thermal pressure, which causes them to expand, is tipped towards the latter. The result is

that post-main sequence stars will be more puffed up, and will have weaker surface gravity, which means that we will detect ever narrower spectral lines. In the most general classification scheme, the luminosity classes will also include the following types of stars: IV: subgiants; III: giants; II: bright giants; I: supergiants.

We also measured the equivalent widths (area under the curve) of the Hα line and noted the presence of emission, which may indicate that the object is a classical Be star or possibly a protostar. Table 1 contains a summary of the observed objects and their resulting derived properties – only the 13 young stars that exhibit Hα absorption are candidates for planet-forming systems.

Analysis:

Three of the observed stars show Hα in emission, one has a mixed profile, and 19 have Hα in absorption. Six of the stars are evolved (luminosity class III or IV) while 17 appear to be main-sequence stars. The main-sequence stars with emission are probable Be stars or Class II protostars. The evolved stars may be B[e] stars with dusty photospheres. It is only the 13 main-sequence stars lacking Hα emission that may have hot circumstellar dust and are candidates for young systems with warm massive dust disks.

Since the 23 stars discussed here do not fully span the color-color space being studied, observing a larger subset of the initial 449 candidates if advisable. Also, in the case of emission line stars, having a larger study set will allow us to test the positive relation between MIR excess and Hα EW suggested in Figure 3. For sources that exhibit this relation it is even more likely that the MIR excess is caused by the presence of ionized gas around the star.

Finally, as was noted before, there could be PAH contributions to the MIR excess. Since our criterion for MIR excess was based on the [4.5] – [8.0] color the risk of excess emission due to PAHs is reduced, but to eliminate it we should look at the [4.5] – [24.0] color when 24μm photometry becomes available.

Conclusions:

- The majority of our objects (19 stars) show Hα in absorption, effectively ruling out gaseous ionized disks, such as in classical Be stars, as the source of the MIR excesses.

- Figure 3 shows that the objects with the largest MIR excesses (i.e., greatest [4.5]-[8.0] colors) have the strongest emission lines, suggesting that, in stars with emission lines, free-free emission in an ionized disk is the likely cause of the MIR excess.

- Circumstellar dust is the probable cause of the MIR excess for the sources that show Hα in absorption. These objects may be dusty evolved stars in some cases (6 sources), while others (13 sources) are good candidates for young, near-main-sequence star systems harboring dust disks, possibly debris-disk systems.

Sources:

Benjamin, R., et al. 2003, PASP, 115, 953
Brackett, F., 1922, ApJ, Volume 56, No. 3, p. 154-161
Hillenbrand et al. 1992, ApJ, 397, 613
Hartmann et al. 2005, ApJ, 628, 881
Keenan, P., et al. 1973, ARAA 11:29-50
Mulas, G., et al. 2005, Journal of Physics: Conference Series 6, p. 217-222
Norton, A. et al. 2004, Cambridge University Press, “Observing the Universe”
Silva, D. & Cornell, M. 1992, ApJ SS, vol. 81, p. 865-881
Uzpen, B. et al. 2005, ApJ, 629:512-525
Uzpen, B. Et al. 2007, ApJ, 658:1264-1288

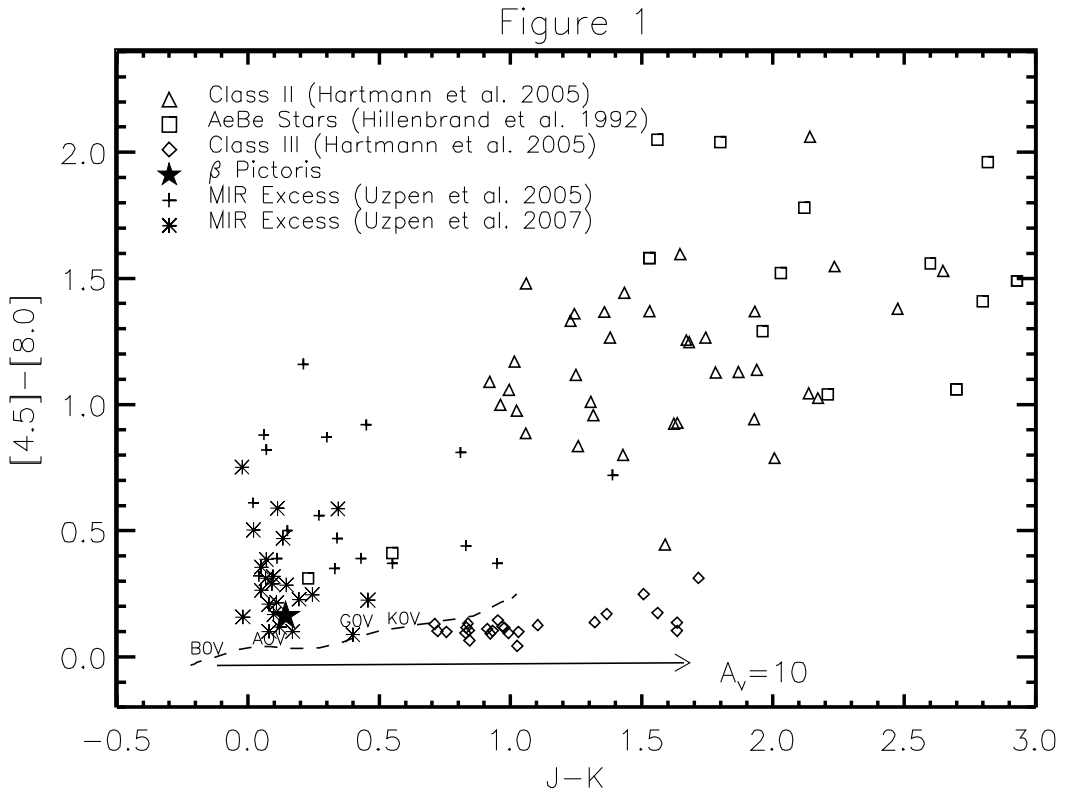

Figure 1: Shows the *J-K* versus [4.5]-[8.0] colors for solarmass Class II protostars (triangles), 2-4 solar mass Class II protostars, also called Herbig AeBe stars (squares), and Class III solar mass protostars (diamonds). Beta Pictoris, a warm A5V star with a debris disk, is denoted by a filled star. Asterisks and pluses show IR excess stars investigated by Uzpen et al. (2005, 2007). The dashed line shows the main sequence. The vector given for A(V)=10 indicates the direction, in which sources will shift on the diagram in the presence of 10 magnitudes of visual extinction (reddening). Reddenning is the process of making stars look redder due to interstellar particles scattering, or absorbing and re-emitting stellar light. The more material there is between us and a star, the redder that star will appear to us.

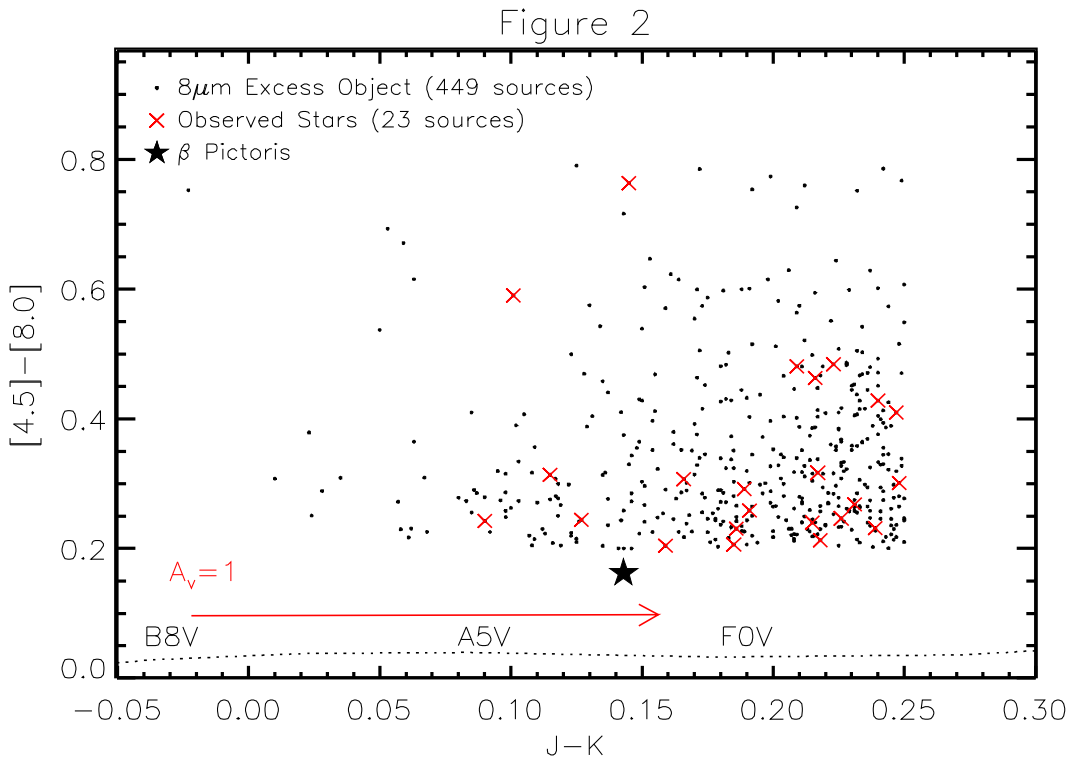

Figure 2: A plot of *J-K* versus [4.5]-[8.0] color for the 449 GLIMPSE sources we selected with -0.03 < J-K < 0.25 and 0.2 < [4.5]-[8.0] < 0.8, shown as dots. Stars in this color box have similar color to Beta Pictoris (denoted by a filled star) and may be pre-main sequence stars undergoing disk clearing and approaching the main sequence or warm debris disks like Beta Pictoris. Classical Be stars and evolved intermediate-mass stars may also occupy this color space, therefore we collected spectral data (see Fig. 4 and Table 1) to determine the origin of the IR excess for the 23 sources that we studied (marked with 'X'). Also shown are a reddening vector for A(V)=1 and the main sequence (dotted line). The main sequence here is unreddened, therefore all sources fall to the right of their corresponding spectral classes.

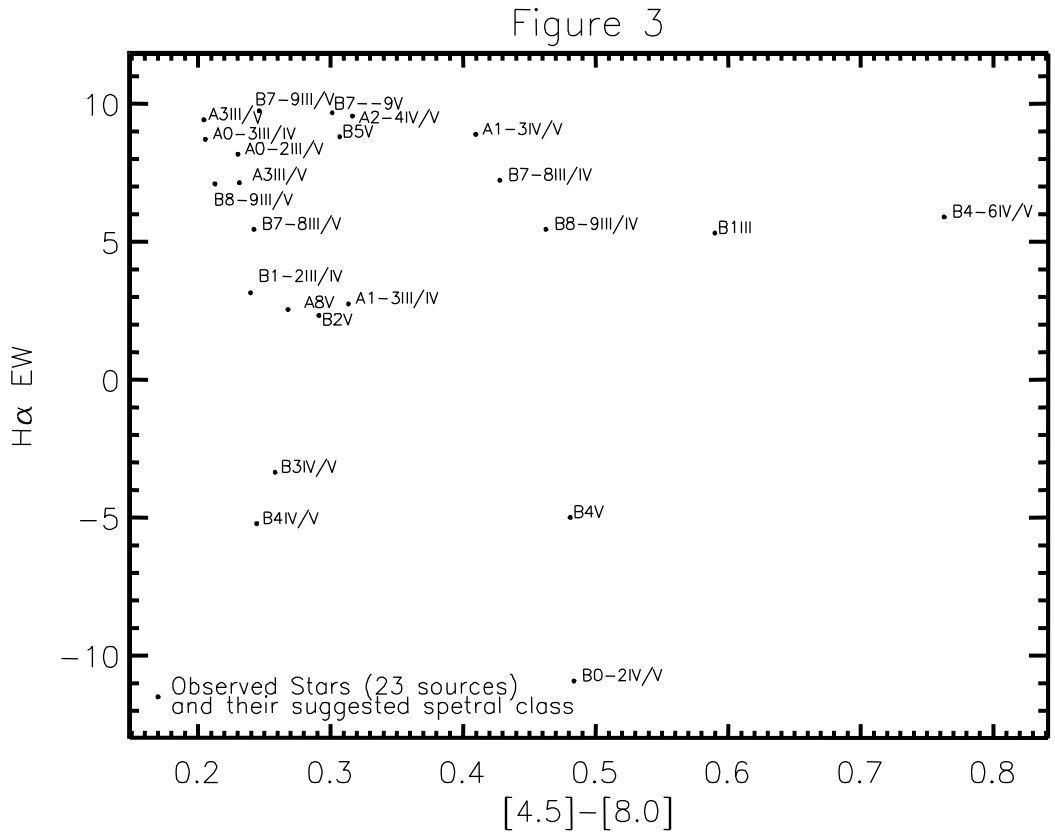

Figure 3: A plot of [4.5]-[8.0] color versus Hα equivalent width (negative values indicate an emission line) for the 23 observed sources (denoted by dots). Each star is plotted along with the spectral and luminosity class that we assigned to it based on WIRO observations. The plot shows that the objects with the largest IR excesses (i.e., reddest [4.5]-[8.0] colors) have the strongest emission lines (the stronger a line is, the larger the magnitude of its EW will be), suggesting that, in stars with emission lines, free-free emission in an ionized disk (one having gas) is the likely cause of the IR excess.

Figure 4

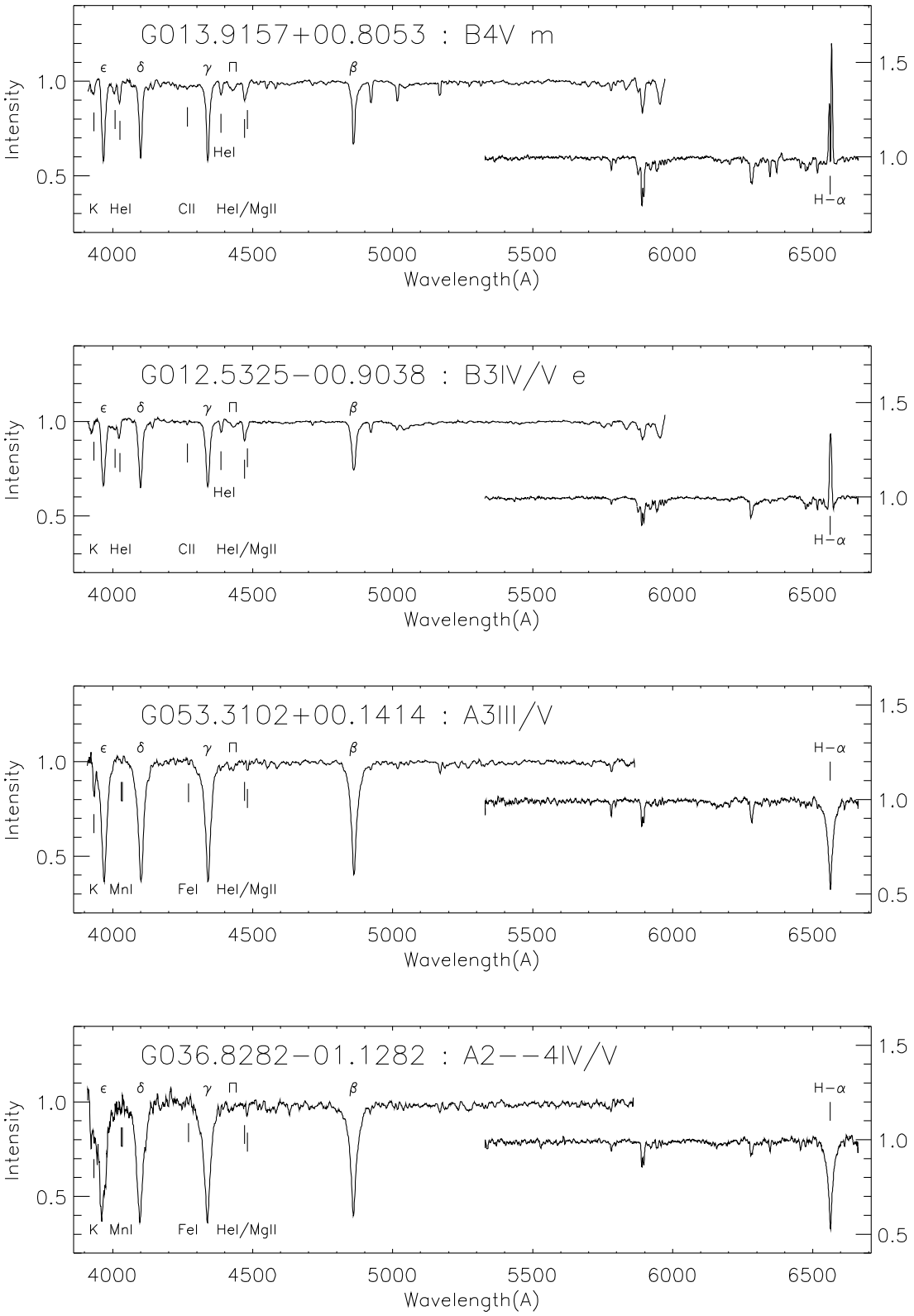
G013.9157+00.8053 : B4V m
G012.5325−00.9038 : B3IV/V e
G053.3102+00.1414 : A3III/V
G036.8282−01.1282 : A2−−4IV/V
Intensity
Wavelength(A)
ε
δ
γ
Π
β
H−α
K
HeI
CII
HeI/MgII
MnI
FeI

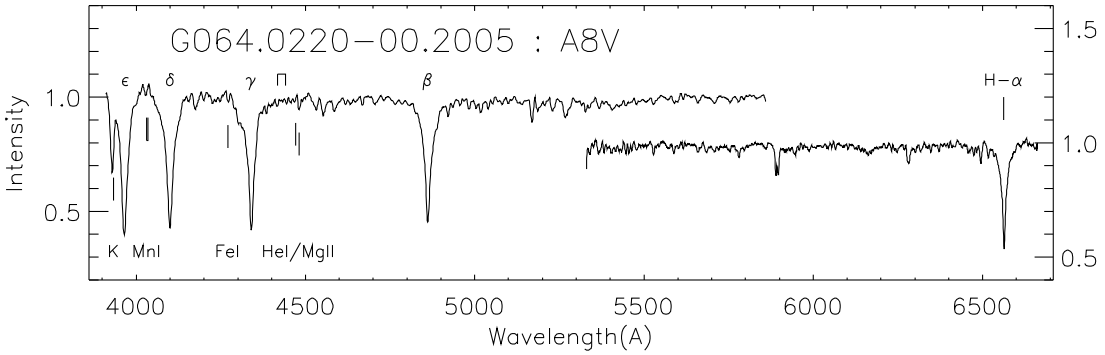
G064.0220−00.2005 : A8V
ε
δ
γ
Π
β
H−α
K
MnI
FeI
HeI/MgII
Intensity
Wavelength(A)

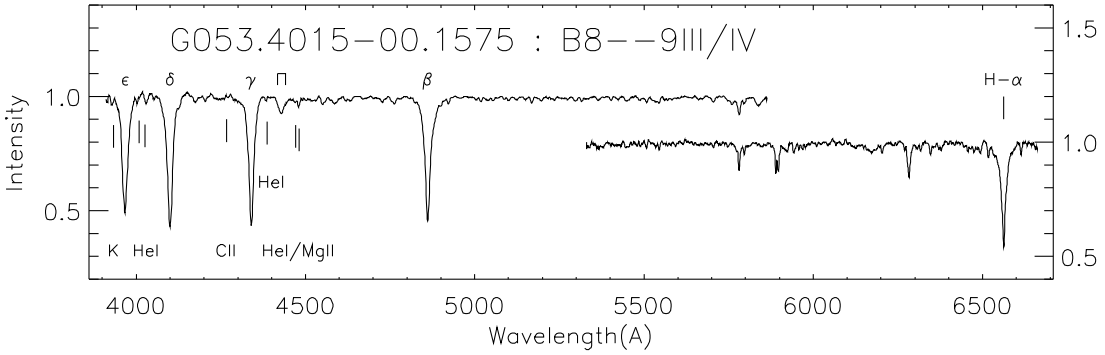
G053.4015−00.1575 : B8−−9III/IV
ε
δ
γ
Π
β
H−α
HeI
K
HeI
CII
HeI/MgII
Intensity
Wavelength(A)

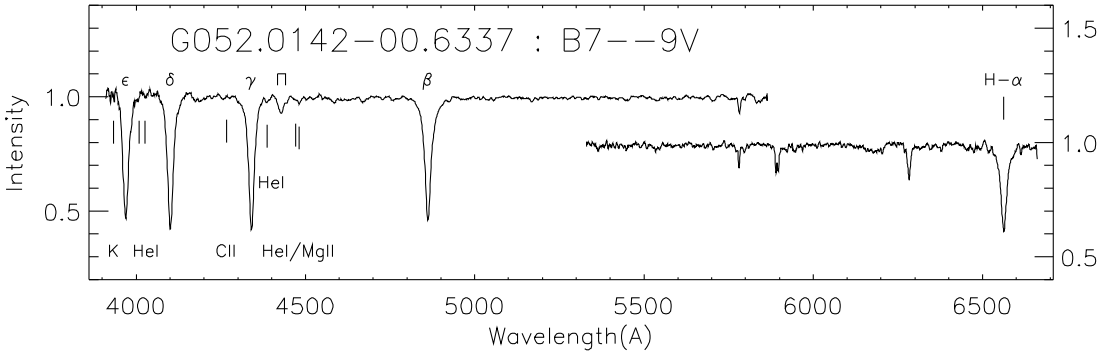
G052.0142−00.6337 : B7−−9V
ε
δ
γ
Π
β
H−α
HeI
K
HeI
CII
HeI/MgII
Intensity
Wavelength(A)

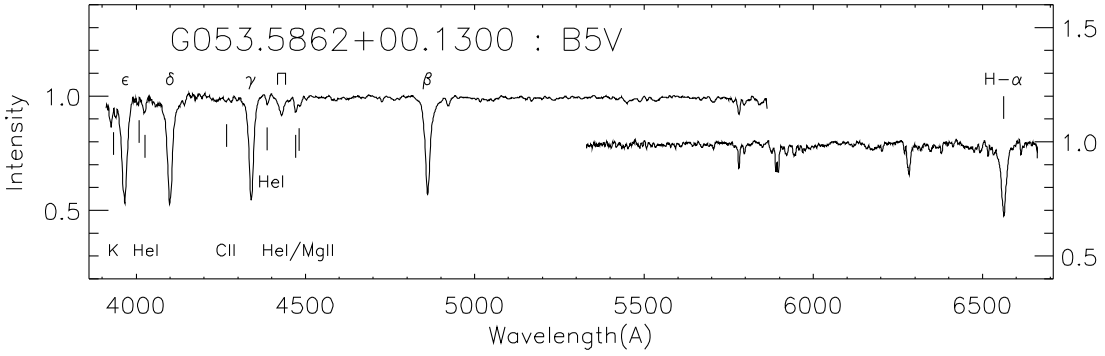
G053.5862+00.1300 : B5V
ε
δ
γ
Π
β
H−α
HeI
K
HeI
CII
HeI/MgII
Intensity
Wavelength(A)

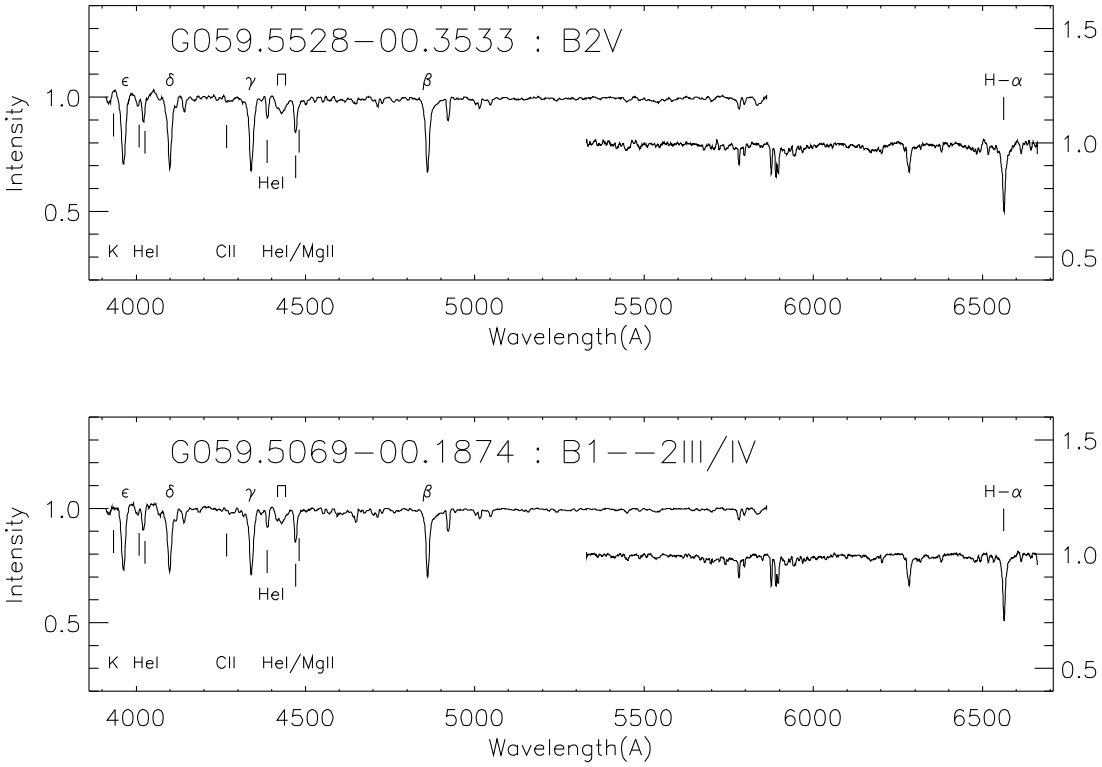

Figure 4: Optical spectra (wavelength vs. intensity) for a representative sample of 10 observed objects. Each star is named after its galactic coordinates, followed by its approximate spectral and luminosity type. Spectral lines relevant to the classification of each source are indicated by vertical marks and by their name, or the name of the element or molecule causing them. The vertical position of most line marks (hydrogen lines are the exception) depends on the strength of the line that they indicate, thereby allowing us to compare the relative strengths of various lines – a criterion used for classification. The five most prominent lines are the Balmer series of hydrogen, starting with Hα at about 6563 Å and ending with Hε at about 3970 Å.

Figure 5

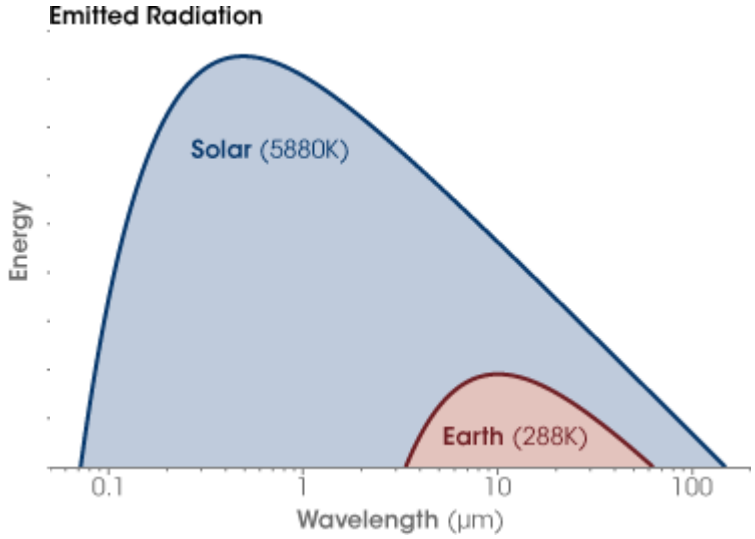

Figure 5: Black body emission curves that approximate the strength of emission at different wavelengths for the Sun and the Earth. Hotter black bodies emit more light at shorter wavelengths, thus the resulting spectral energy distributions. The graph is courtesy of Robert Simmon at the NASA Earth Observatory. http://earthobservatory.nasa.gov/Study/ArcticReflector/Images/black_body_log_log_rt.gif

Table 1

NAME	J mag.	J-K	[4.5]-[8.0]	Spectral Type	Hα profile	Hα EW (Ang)
G011.7710+00.7428	10.36	0.15	0.76	B4-6IV/V	absorption	5.89±0.08
G012.2321-00.1289	9.76	0.09	0.24	B7-8III/V	absorption	5.44±0.06
G012.4488-01.0225	9.91	0.16	0.20	A3III/V	absorption	9.42±0.12
G012.5325-00.9038	9.92	0.19	0.26	B3IV/V	emission	-3.37±0.03
G013.1871-00.6730	9.22	0.13	0.24	B4IV/V	emission	-5.23±0.03
G013.9157+00.8053	9.97	0.21	0.48	B4V	mixed	-5.00±0.50
G036.8282-01.1282	9.98	0.25	0.41	A2-4IV/V	absorption	8.88±0.14
G044.1564-00.1019	10.99	0.22	0.32	A0-3III/IV	absorption	9.56±0.05
G046.6761+00.7553	10.46	0.19	0.21	B8-9III/V	absorption	8.71±0.08
G049.0294-01.0909	10.21	0.22	0.21	B7-9III/V	absorption	7.10±0.09
G051.2198+00.2156	10.85	0.23	0.25	A0-2III/V	absorption	9.74±0.06
G052.0142-00.6337	10.81	0.19	0.23	B7--9V	absorption	8.17±0.11
G053.3102+00.1414	10.80	0.25	0.30	A3III/V	absorption	9.66±0.04
G053.4015-00.1575	10.40	0.24	0.23	B8-9III/IV	absorption	7.13±0.05
G053.5862+00.1300	10.75	0.22	0.46	B5V	absorption	5.44±0.07
G054.8416+00.1924	10.29	0.17	0.31	A1-3III/IV	absorption	8.79±0.20
G059.5069-00.1874	9.85	0.11	0.31	B1-2III/IV	absorption	2.75±0.03
G059.5528-00.3533	10.33	0.21	0.24	B2V	absorption	3.14±0.01
G063.3831+00.3244	10.61	0.19	0.29	B1III	absorption	2.32±0.05
G063.7242-01.0033	10.54	0.10	0.59	B7-8III/IV	absorption	5.31±0.06
G064.0220-00.2005	10.81	0.24	0.43	A8V	absorption	7.22±0.04
G064.2692-00.0280	10.22	0.23	0.27	B0-2IV/V	absorption	2.53±0.05
G064.7559+00.5491	10.46	0.22	0.48	B5-6V	emission	-10.93±0.02

Table 1: A summary of the observed objects and their resulting derived properties. Each star is named after its galactic coordinates. We have also shown the *J-K* and [4.5]-[8.0] color, the *J* magnitude (we selected dim stars *J*~10), the approximate spectral and luminosity type, and the Hα profile and equivalent width (errors were obtained after the averaging of several measurements) for each source.